Algorithm Theoretical Baseline Document - Polar Ocean

Lars Stenseng
ATBD, Version 0.9
May 7, 2014

Algorithm Theoretical Baseline Document - Polar Ocean

Lars Stenseng
National Space Institute
ATBD, Version 0.9, Kgs. Lyngby, May 7, 2014

Document history

Version	Date	Affected sections	Comment
0.9	May 7, 2014		Initial version

Table 1: Document history

Contents

IV

1 Introduction

This document concerns the theoretical development and operational implementation of the system for classification and retracking of SAR mode altimeter waveforms obtained over Polar oceans where sea-ice is occurring. The primary input to the system is the L1b and L2 products from the ESA Baseline-B processing, but additional L2 data have been considered as well.

2 Introduction to the Polar Ocean

For many surfaces, e.g. the open ocean, the surface can be assumed to be close to a diffuse reflector when observed from within a few degrees from nadir. These surfaces will reflect and spread the incoming radar energy almost equally in all directions, see Figure 1. A study of SAR altimetry data from the Airborne SAR/Interferometric Radar Altimeter System (ASIRAS) over open ocean show that within $\pm 6°$ from nadir the return power is primarily attenuated by the antenna pattern (Stenseng, 2009).
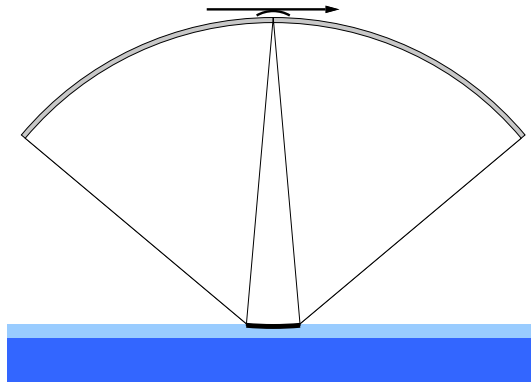
Figure 1: Reflected power from a diffuse surface e.g open ocean or a sea-ice floe.

In the sea-ice covered part of the Polar Ocean is a combination of several different surface types i.e. smooth young ice, rough old ice, pressure ridges, sea-ice melange, leads and open water. Here the primarily focus will be on the leads which can be used for deriving the sea level height. Secondary the open water and diluted sea-ice melange will be discussed.

Lead is typical defined as a fracture, with open water or thin newly formed ice, in the sea-ice cover with width up to several hundreds of meters

and reaching several kilometers in lengths. Since the sea-ice cover attenuates the ocean waves, the thin ice or water surface in the lead will usually be smooth with only small wind generated waves. This smooth surface will give a specular return where most power is reflected to the point closest to the burst position that is perpendicular to the water surface i.e. the nadir pointing beam, see Figure 2.

(a) In front of the lead power is primarily reflected forward, away from the satellite.

(b) Over the lead power is primarily reflected back to the satellite.

(c) Past the lead power is primarily reflected backwards, away from the satellite.
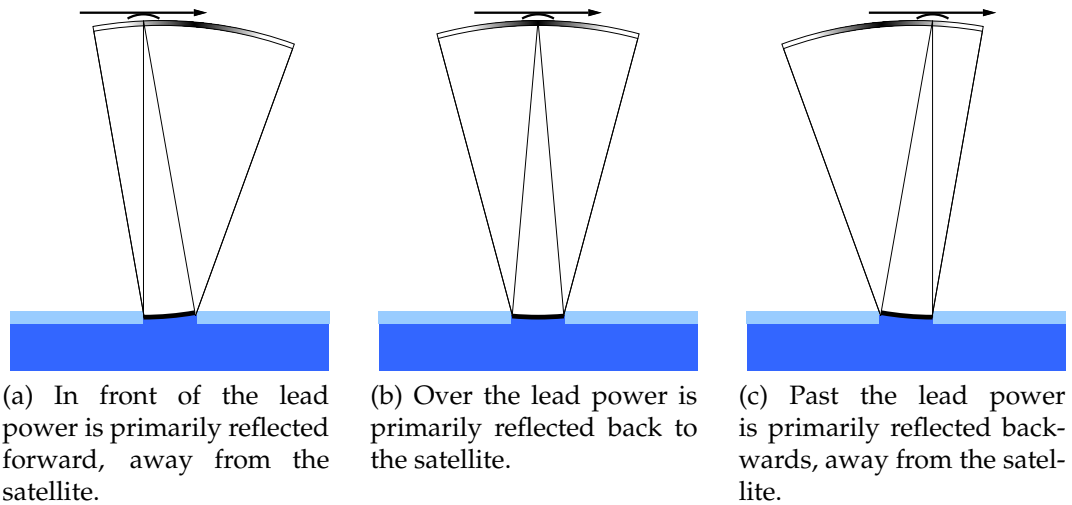
Figure 2: Reflected power from a lead observed from three different positions.

3 Algorithm Description

The major challenges in obtaining sea surface height estimates in the Polar Ocean is many; the limited amount of sea-ice leads, areas with sea-ice melange, retracking of extreme peaky waveforms and off-nadir returns.

3.1 Overview of algorithm flow
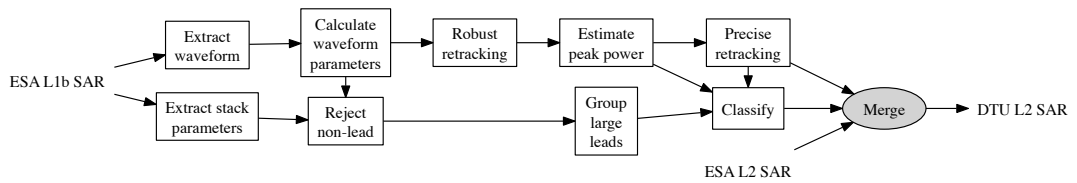
Figure 3: Overview of algorithm flow.

3.2 Determine a power benchmark for the retracker

The first step is to identify the bin of maximum power which will be close to the center of the peak. However, the very narrow peak from the specular reflection might not be coincident with a bin position (see Figure 4) and therefore a more stable peak power must be found.

To obtain a stable value for the power benchmark (P_b) the bin position with maximal power (m) is found and the benchmark power is then calculated as the average of the maximal power and the power of two bin on each side of the maximal bin position, see Equation 1. It should be emphasized that the derived power benchmark is not an estimate of the true peak and should therefore not be used to derive a surface roughness parameter like σ_0.

$$P_b = \frac{1}{5} \sum_{i=m-2}^{m+2} p_i \tag{1}$$

(a) Maximum power coincident with a sample bin (black) overlayed with a fitted Gaussian (red).

(b) Maximum power between with two sample bins (black) overlayed with a fitted Gaussian (red).
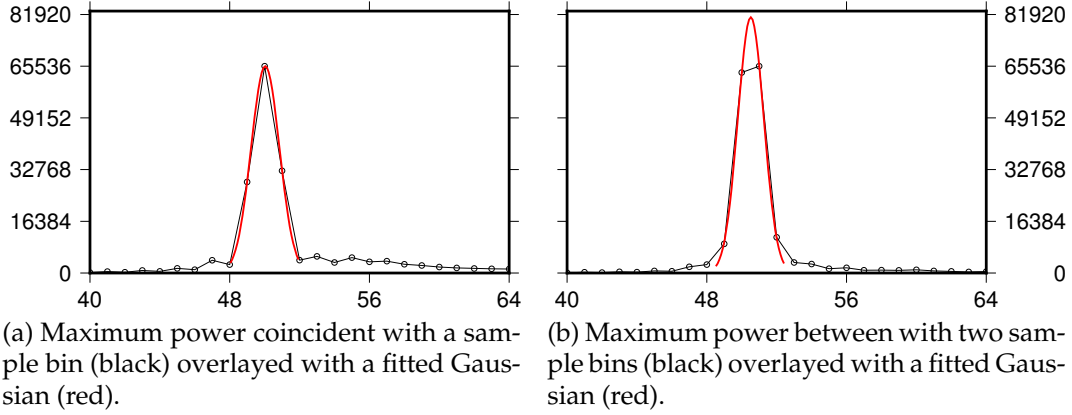
Figure 4: Cutoff of maximal peak due to bin offset relative to maximal power.

3.3 Performing the retracking

The retracking of the waveforms is performed using a simple leading edge threshold retracker similar to that of Davis (1997). The threshold value F_T is chosen between 0 and 1 and indicates the fraction of the power benchmark to be used for the retracking point. To begin with the first bin position (j) with power higher than or equal to $F_T \cdot P_b$ is found and a linear interpolation between bin j and bin $j-1$ is performed to obtain the fraction of a bin where the threshold power is found. Finally the epoch is derived, in bin counts, by adding $j-1$ to the fraction as described in Equation 2.

$$E = \frac{F_T \cdot P_b - p_{j-1}}{p_j - p_{j-1}} + j - 1 \qquad (2)$$

3.4 Identify leads (Classification)

The classification is primarily based on a set of parameters describing the morphology of the waveform and the power distribution in the individual looks in the stack. The parameters describing the power distribution is taken directly from the ESA Baseline-B L1b product and the parameters describing the morphology is described in the following. Furthermore, as described above the ESA Baseline-B L2 product is merged into the DTU dataset which allows a direct comparison of the ESA Baseline-B classification of the individual waveforms.

A classic parameter for identification of specular returns is the Pulse

peakiness (*PP*), which determines the ratio between the peak power and the integrated power in the waveform (Laxon, 1994; Peacock and Laxon, 2004). In the classical formulation the first five samples are discarded to avoid wrap around effects and the ratio is scaled using the nominal tracking point bin. A pulse peakiness value is available in the ESA Baseline-B L2 product but the used formulation is unknown and results in values exceeding 500 as opposed to the classical values not exceeding 1. Equation 3 gives the formulation used in the DTU classification.

$$PP = \frac{65535}{\sum_{i=0}^{127} p_i} \tag{3}$$

To further characterize the peak a Gaussian (see Equation 4) is fitted to the most powerful bin including two bins on each side similar to approach by Armitage and Davidson (2014). This will give additional information about the peak geometry and aid the identification of contaminated lead returns.

$$G_i = A_g \cdot \exp\left(-\frac{(i - E_g)^2}{2 \cdot W_g^2}\right) \tag{4}$$

By rearranging the classical radar equation (e.g. Skolnik (2001)), tacking the Earths curvature into account, and using the power estimated by the Gaussian fitted to the peak, a simplified version of σ_0 can be estimated as following:

$$\sigma_0 = 40 \cdot log_{10}(h) + 10 \cdot log_{10}\left(\frac{R_e}{R_e + h}\right) + 10 \cdot log_{10}\left(\frac{P_u}{P_{Tx}}\right) + C_{\sigma_0} \tag{5}$$

where P_u is the power in Watts derived from A_g, P_{Tx} is the transmitted power and C_{σ_0} is a constant accounting for all other losses which will be assumed to be constant.

3.4.1 Selecting lead returns

Using the stack standard deviation delivered in the ESA L1b product and the calculated pulse peakiness, returns with high stack standard deviation or low pulse peakiness are rejected as being non-leads. Next the remaining possible lead candidates are grouped if there are no more than two non-lead samples between possible lead candidates. In large groups the return with highest σ_0 and a stack center position close to the true stack center for each subgroup of five returns is selected as representative for the subgroup.

Single lead returns are selected if the pulse peakiness is very high, the stack standard deviation is low and the σ_0 is high. The values for the thresholds on these parameters can be relaxed if the number of lead returns is more important that the precision. This could be relevant in areas with permanent high sea-ice concentration and therefore fewer and smaller leads.

4   Constrains and limitations

The primary constrain of the presented algorithm is the natural variability in the number, size and cross-track location of the leads. Due to the nature of the sea-ice the number of leads changes both with region and season, allowing only few leads in the dense sea-ice north of Greenland and Canada and further limiting the general number and size of leads in the winter season.

The random cross-track location of the leads relative to the nadir point will introduce a negative bias in the height estimate of the water surface as the observed slant range to the specular lead will be grater than the range to the nadir point. The filtering of lead return groups will to some degree reduce the negative bias.

Finally the limited bandwidth of the radar pulse will introduce noise in the height estimates as the highly specular peak is only captured in a very few gates (down to three gates) even after resampling at the power Nyquist frequency (i.e. zero padding the complex signal by size factor of two)

Bibliography

Armitage, T. W. K. and Davidson, M. W. J. (2014). Using the interferometric capabilities of the esa cryosat-2 mission to improve the accuracy of sea ice freeboard retrievals. *IEEE Transactions on Geoscience and Remote Sensing*, 52(1):529–536.

Davis, C. H. (1997). A robust threshold retracking algorithm for measuring ice-sheet surface elevation change from satellite radar altimeters. *IEEE Transactions on Geoscience and Remote Sensing*, 35(4):974–979.

Laxon, S. W. (1994). Sea ice extent mapping using ERS-1 radar altimeter. *EARSeL Advances in Remote Sensing*, 3(2):112–116.

Peacock, N. R. and Laxon, S. W. (2004). Sea surface height determination in the arctic ocean from ers altimetry. *Journal of Geophysical Research*, 109.

Skolnik, M. (2001). *Introduction to radar systems*. McGraw-Hill.

Stenseng, L. (2009). SAMOSA WP8 technical note. validation using airborne asiras data. Technical report, DTU-Space.

A Symbols

A_g Peak power in Gaussian fit
C_{σ_0} Constant between estimated σ_0 and true σ_0
E Retracked epoch (expressed in bins)
E_g Epoch of Gaussian peak (expressed in bins)
F_T Threshold value for threshold retracker
G_i Power in bin i of the fitted Gaussian
h Satellite altitude
i Integer index
j Integer index
m Bin number with maximal power in the waveform
P_b Power benchmark for threshold retracker
p_i Power in bin i of the waveform
PP Pulse peakiness value
$P_T x$ Transmitted power in Watts
P_u Estimated received power in Watts
R_e Earth mean radius (6371 km)
W_g Width of fitted Gaussian (expressed in bins)
σ_0 Backscatter coefficient

B Acronyms and Abbreviations

ASIRAS	Airborne SAR/Interferometric Radar Altimeter System
ATBD	Algorithm Theoretical Baseline Document
DTU Space	National Space Institute, Technical University of Denmark
ESA	European Space Agency